AD-A064 763 UTAH UNIV SALT LAKE CITY DEPT OF CHEMISTRY F/G 11/6
RATES OF RAPID CHEMICAL REACTIONS.(U)
JAN 79 E M EYRING AFOSR-77-3255

UNCLASSIFIED AFOSR-TR-79-0088 NL

| OF |
AD
A064763

END
DATE
FILMED
4-79
DDC

FINAL TECHNICAL REPORT TO THE

AIR FORCE OFFICE OF SCIENTIFIC RESEARCH,

CHEMICAL DIRECTORATE

Project Title:	RATES OF RAPID CHEMICAL REACTIONS
Institution:	University of Utah, Salt Lake City, Utah
Principal Investigator:	Dr. Edward M. Eyring
Grant Award Number:	AFOSR 77-3255
Report Period:	February 1, 1977 to November 30, 1978

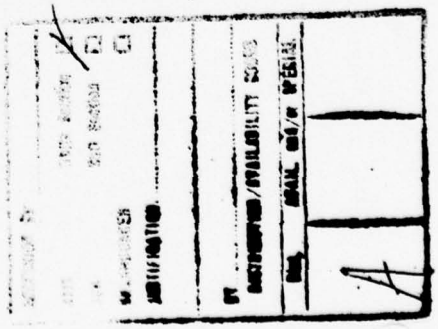

SECURITY CLASSIFICATION OF THIS PAGE (When Data Entered)

REPORT DOCUMENTATION PAGE	READ INSTRUCTIONS BEFORE COMPLETING FORM
1. REPORT NUMBER: AFOSR-TR-79-0088	2. GOVT ACCESSION NO. / 3. RECIPIENT'S CATALOG NUMBER
4. TITLE (and Subtitle): Rates of Rapid Chemical Reactions.	5. TYPE OF REPORT & PERIOD COVERED: Final Technical Report. 1 Feb 1977 to 30 Nov 1978
	6. PERFORMING ORG. REPORT NUMBER
7. AUTHOR(s): Edward M. Eyring	8. CONTRACT OR GRANT NUMBER(s): AFOSR-77-3255
9. PERFORMING ORGANIZATION NAME AND ADDRESS: Department of Chemistry, University of Utah, Salt Lake City, Utah 84112	10. PROGRAM ELEMENT, PROJECT, TASK AREA & WORK UNIT NUMBERS: 61102F 2303/A2 A2
11. CONTROLLING OFFICE NAME AND ADDRESS: Directorate of Chemical Sciences, Air Force Office of Scientific Research, Bolling, AFB, DC 20332	12. REPORT DATE: 22 January 1979
	13. NUMBER OF PAGES: 30
14. MONITORING AGENCY NAME & ADDRESS (if different from Controlling Office): 34 p.	15. SECURITY CLASS. (of this report): Unclassified
	15a. DECLASSIFICATION/DOWNGRADING SCHEDULE

16. DISTRIBUTION STATEMENT (of this Report)

Approved for public release: distribution unlimited.

17. DISTRIBUTION STATEMENT (of the abstract entered in Block 20, if different from Report)

18. SUPPLEMENTARY NOTES

19. KEY WORDS (Continue on reverse side if necessary and identify by block number)

corrosion	reaction rates	piezoelectric detector
titanium	Fourier transform	Hadamard transform
perfluoropolyether	photoacoustic spectroscopy	activation energy
lubricant	Michelson interferometer	argon-ion laser

20. ABSTRACT (Continue on reverse side if necessary and identify by block number)

A rate and mechanism study of the corrosion of titanium metal by a hot perfluoropolyether lubricant has been carried out by a laser beam reflectance technique. A Fourier transform photoacoustic spectroscopy (FTPAS) technique has been developed that is potentially capable of producing absorption spectra of opaque surfaces at infrared wavelengths. FTPAS was not found suitable for studying corrosion of titanium because of thermal problems with the piezoelectric detector. Some homogeneous solution kinetic studies of reactions in water, acetonitrile and methanol were carried out also.

DD FORM 1 JAN 73 1473 400 430 Unclassified

SUMMARY

The primary objective of this research was the development of techniques to investigate the kinetics and mechanism of the corrosion of titanium metal by a hot perfluoropolyether lubricant. The method originally expected to be most appropriate was photoacoustic spectroscopy using piezoelectric detection. Such an apparatus was found to be satisfactory for measuring the visible absorption spectrum of static solid systems such as a neodymium(III) glass laser rod. A Fourier transform photoacoustic spectrometer was assembled from a Michelson interferometer and a dedicated minicomputer with the expectation that it would be more suitable for measuring fairly rapid changes in the visible absorption spectrum of a corroding surface. However, neither type of photoacoustic spectrometer proved effective in observing titanium corrosion by the hot perfluoropolyether. A steep thermal gradient in a titanium rod, one end of which was bathed with lubricant at 270°C while the other end was in contact with the piezoelectric (barium titanate) detector at room temperature, posed intractable noise problems for either type of photoacoustic spectrometer.

A CW argon-ion laser was then adapted for a reflectance study of the titanium corrosion reaction. The rate of corrosion is a strong function of the amount of oxygen available in and above the hot lubricant. The degradation of the lubricant and resultant formation of TiF_3 on the titanium surface is accelerated by TiF_3 corrosion products but is unaffected by the intense laser illumination. From kinetic data covering the 215 to 270°C temperature range an activation energy for the overall corrosion process of 19 kJ/mole was found. When the titanium surface is carefully polished to remove all traces of corrosion products an extended induction time precedes the exponential corrosion process.

The most significant accomplishment to emerge from these studies was the reduction to practice of a Fourier transform photoacoustic spectrometer that ap-

pears to be adaptable to transient mid-infrared surface absorption spectral measurements.

Incidental byproducts of this research were complex ion formation and proton transfer kinetic studies (in liquid water, methanol, and acetonitrile) carried out primarily by unpaid foreign visitors to our laboratory on minicomputer controlled ultrasonic absorption and electric field jump equipment paid for by previous AFOSR grants.

DISCUSSION

The goals of this twenty-two month research period were basically two fold: 1) We sought a better understanding of the kinetics and mechanism of the corrosion of titanium metal by a hot perfluoropolyether lubricant (DuPont PR-143); and 2) We proposed to adapt photoacoustic spectroscopy (PAS) to the measurement of fast transients in the visible absorption spectrum of a corroding surface.

The results achieved under our first objective have not yet been submitted for publication. Difficulties with a noisy PAS signal arising from a steep thermal gradient in the titanium metal rod between the corroding titanium surface (at 270°C) and the piezoelectric transducer (at room temperature) forced us to abandon PAS measurements of titanium corrosion. We resorted instead to the use of a laser beam reflectance technique to obtain our titanium corrosion kinetic data. These experiments are described in Appendix I of the present technical report. The most interesting features of the results are an expected strong dependence on the amount of oxygen present in and above the hot lubricant and an unexpectedly strong dependence of the corrosion rate on the presence of traces of TiF_3 corrosion products on the titanium metal surface.

In the early part of the grant period (February-June, 1977) we perfected our measurements of the visible absorption spectrum of neodymium(III) doped laser glass using PAS and a piezoelectric barium titanate detector. These results were

published in April, 1978 (see publication no. 5 below). In September, 1977 we conceived the idea of a Fourier transform photoacoustic spectrometer that could do either of two things: improve the signal to noise ratio for a given observation time or shorten the observation time required to achieve a given signal to noise ratio. At the time, the motivation for assembling such an instrument was two-fold: it might aid us in getting PAS data on the corrosion of titanium by hot lubricant and it might also point the way to a workable infrared PAS that would have far wider applicability than the visible photoacoustic spectrometers that had then gone into commercial production.

We completed a prototype Fourier transform photoacoustic spectrometer in April, 1978. A manuscript reporting the measurement of the photoacoustic spectrum of neodymium(III) doped laser glass with this new instrument was subsequently published (see publication no. 7 below). Since we found we could not use FTPAS to follow the corrosion of titanium by hot lubricant (because of noise associated with a thermal gradient in the system), comparatively little additional work has been done to improve the prototype FTPAS instrument. Appendix II is an up to date description of our FTPAS instrument and its manner of operation essentially as we have treated it in publication no. 11 below. We believe that such a Fourier transform instrument can be adapted for studies of surfaces at infrared wavelengths and are seeking funds to explore this possibility from several new research sponsors.

Foreign visitors to our laboratory (Drs. F. A. Vazquez and Licesio Rodriguez from Spain and Dr. Frank Strohbusch from Germany) were largely responsible for most of the other papers acknowledging financial assistance of this grant that are listed below. These visitors drew stipends from their respective governments but used AFOSR purchased equipment (an ultrasonic absorption spectrometer, minicomputer, and an electric field jump relaxation method apparatus) to complete

these kinetic studies of fast chemical reactions occurring in homogeneous solutions. The studies involving crown ether kinetics (references 1, 3, 4, 6, and 10 below) are potentially interesting in connection with liquid membrane separations of radioactive isotopes from nuclear reactor wastes.

Publications Acknowledging AFOSR Support Appearing Since 1 February 1977

1. "Ultrasonic Absorption Kinetic Studies of the Complexation of Aqueous Li^+, Na^+, Rb^+, $T\ell^+$, Ag^+, NH_4^+, and Ca^{2+} by 18-Crown-6," G. W. Liesegang, M. M. Farrow, F. A. Vazquez, N. Purdie, and E. M. Eyring, J. Am. Chem. Soc., 99, 3240 (1977).

2. "Equilibrium and Kinetic Investigation of Salt-Cycloamylose Complexes," R. P. Rohrbach, L. J. Rodriguez, Edward M. Eyring, and J. F. Wojcik, J. Phys. Chem., 81, 944 (1977).

3. "Kinetic Studies of the Complexation of Monovalent Sodium, Potassium, Rubidium, Thallium, and Silver Cations by Aqueous 15-Crown-5," L. J. Rodriguez, G. W. Liesegang, R. D. White, M. M. Farrow, N. Purdie and E. M. Eyring, J. Phys. Chem., 81, 2118 (1977).

4. "Kinetic Studies of Complexation of Divalent Strontium, Barium, Lead, and Mercury Cations by Aqueous 15-Crown-5 and 18-Crown-6," L. J. Rodriguez, G. W. Liesegang, M. M. Farrow, N. Purdie, and E. M. Eyring, J. Phys. Chem., 82, 647 (1978).

5. "Piezoelectric Detection of Photoacoustic Signals," M. M. Farrow, R. K. Burnham, M. Auzanneau, S. L. Olsen, N. Purdie, and E. M. Eyring, Applied Optics, 17, 1093 (1978).

6. "Dynamics of a Conformational Change in Aqueous 18-Crown-6 by an Ultrasonic Absorption Method," G. W. Liesegang, M. M. Farrow, L. J. Rodriguez, R. K. Burnham, E. M. Eyring, and N. Purdie, Int. J. Chem. Kinetics, 10, 471 (1978).

7. "Fourier-Transform Photoacoustic Spectroscopy," M. M. Farrow, R. K. Burnham, and E. M. Eyring, Appl. Phys. Lett., 33, 735 (1978).

8. "Kinetics of Proton Transfer Between Picric Acid and Two Azo Indicators in Acetonitrile," F. Strohbusch, D. B. Marshall, and E. M. Eyring, J. Phys. Chem., 82, 2447 (1978).

9. "Optical Ultrasonic Techniques," E. M. Eyring and M. M. Farrow, in *New Applications of Chemical Relaxation Spectrometry and Other Fast Reaction Methods in Solution*, E. Wyn-Jones, ed., D. Reidel Publishing Co., Dordrecht, Holland, in press.

10. "Crown Ether Reaction Kinetics," E. M. Eyring, M. M. Farrow, L. J. Rodriguez, L. B. Lloyd, R. P. Rohrbach, and E. L. Allred, loc. cit., in press.

11. "Fourier Transform Photoacoustic Spectroscopy," M. M. Farrow, R. K. Burnham, and E. M. Eyring, loc. cit., in press.

12. "Reaction Rate Measurements in Solution on Microsecond to Subnanosecond Time Scales," N. Purdie, E. M. Eyring, and L. J. Rodriguez, in *Chemical Experimentation Under Extreme Conditions*, B. W. Rossiter, ed., Interscience Publishers, New York, N.Y., in press.

13. "The Dissociation Kinetics of Picric Acid and Dipicrylamine in Methanol. A Steric Effect on a Proton Transfer Rate," F. Strohbusch, D. B. Marshall, F. A. Vazquez, A. L. Cummings, and E. M. Eyring, J. Chem. Soc. Faraday I, accepted for publication subject to minor revision.

14. "Titanium Corrosion by a Hot Perfluoropolyether," W. L. Chandler, L. B. Lloyd, M. M. Farrow, R. K. Burnham, and E. M. Eyring, in preparation.

Appendix I

TITANIUM CORROSION BY A HOT PERFLUOROPOLYETHER*

by

WAYNE L. CHANDLER, LINDSAY B. LLOYD, MICHAEL M. FARROW†,
ROGER K. BURNHAM, AND EDWARD M. EYRING

Department of Chemistry
University of Utah
Salt Lake City, Utah 84112

ABSTRACT

The kinetics and mechanism of titanium corrosion by Krytox MLO-71-6 are reported. The rate of corrosion is found to be dependent on the presence of molecular oxygen in the environment. For titanium corrosion to occur the lubricant chains must first break down into smaller reactive molecules. This degradation process is accelerated by TiF_3 corrosion products on the metal surface, thus giving rise to a chain mechanism. The corrosion is not promoted by intense CW laser illumination at λ = 514 nm.

INTRODUCTION

Perfluoropolyethers have enjoyed some success as replacements for more conventional lubricants in high temperature environments such as jet aircraft engines. They tend, however, to corrode steel and titanium metal surfaces at temperatures of 204 to 410°C (400-770°F), and a micro-oxidation technique has been used to investigate the mechanism of the corrosion process.[1] Further work has been done on various types of corrosion inhibition additives.[2-4]

The kinetics of corrosion of titanium metal by a DuPont perfluoropolyether (Type MLO-71-6 or Krytox) have been explored in the present study by a reflectance technique.

---

*Manuscript received

†Present Address: Office Products Division, IBM Corporation, Boulder, CO 80302

LUBRICANT CORROSION CELL AND REFLECTANCE SPECTROMETER

A high temperature corrosion cell was constructed from Monel (see Fig. 1) which is not corroded by the hot perfluoropolyether. The cell body contains four resistive heating elements capable of raising the cell temperature to 400°C (750°F). The temperature was recorded and controlled either by a Digital Equipment Corp. (DEC) PDP 11/10 minicomputer that monitored power output to the heaters through solid state relays or by hand with a Variac adjustable transformer. In either case ten minutes elapsed as the cell was brought up to the operating temperature of 215 to 270°C (419-518°F) and stabilized there. Cell temperature was monitored with an Omega Model 250 digital platinum resistance thermometer and maintained constant to ±1°F throughout the course of an experiment.

A 1 inch diameter cylindrical hole through the sample cell center accepts a chemically pure titanium metal rod of the same diameter. Before each experiment a squared off face of the cylindrical rod was polished to remove corrosion products of previous experiments. Two polishing protocols were followed: In the one, intended to completely remove all traces of corrosion products, the rod and cell were sanded with carborundum wet-dry paper and the rod face was polished to a high reflectance with a tin oxide abrasive. In the second, intended to leave a trace (<1%) of corrosion products on the face, a finer red rouge abrasive was used.

Teflon O-rings were used to seal the cell around the titanium rod, and a ¼ inch deep well above the titanium rod face was filled with lubricant. Assembled in this manner the cell was then brought up to experimental temperature.

The reflectance light source was a Spectra Physics CW argon-ion laser operating at λ=514 nm. This wavelength is strongly absorbed by the purple corrosion products. While the maximum CW output of the laser is 3 watts, the intensity range used in these experiments was 0.5-1 watt.

Ninety percent of the laser beam passed through a 90/10 beam splitter into the reflectance cell. The remaining 10% was picked up by an RCA 6342 photomultiplier tube (PMT) and served as a continuous light intensity reference. The probe beam passed through the lubricant and illuminated a 1 cm^2 area of the immersed face of the titanium metal rod. The light reflected by the titanium metal surface was detected by a second, identical PMT.

Both photomultiplier outputs (sample and reference) were connected to a DEC LPS-11 Analog to Digital Converter (ADC) which in turn sends the digital data to a DEC LSI-11 microprocessor. The sample voltage was divided by the reference voltage to standardize the data. Signal averaging for 30 sec preceded the recording of each data point. The data points were displayed visually on a Tektronix 4010 graphics terminal.

NITROGEN ATMOSPHERE EXPERIMENTS

For the reflectance measurement under an N_2 atmosphere the cell was placed in a polyethylene glove bag. A glass window was incorporated into the side of the bag to admit the laser light. An opening at the top allowed excess nitrogen and luricant vapors that boiled off to escape. Before the lubricant sample was placed in the cell, the glove bag was flushed for an hour with dry nitrogen to remove atmospheric oxygen. The lubricant sample itself was deoxygenated by bubbling dry nitrogen through it for 4 hours at room temperature. During the corrosion runs a constant stream of nitrogen passed over the surface of the hot lubricant in the cell to flush out the evaporating lubricant. This stream of nitrogen also kept the contents of the glove bag under a constant positive nitrogen pressure.

OXYGEN ATMOSPHERE EXPERIMENTS

Several corrosion experiments were performed with the cell open to the atmosphere and a fast stream of oxygen flushing the surface of the lubricant in the reflectance cell. Before each of these runs, $O_2(g)$ was bubbled through the

lubricant at room temperature for 4 to 6 hours. Other experiments were run under a diminished oxygen atmosphere. In these experiments the cell was open to the air as before but with a stream of dry nitrogen flushing the surface to the lubricant. In these experiments the lubricant was not pretreated by bubbling nitrogen or other gases through it.

EVAPORATION OF THE LUBRICANT

There are two surfaces that reflect light in the lubricant cell. One is the titanium metal itself, the other is the surface of the lubricant. By angling the incident laser illumination the two reflections may be separated and the reflection from the titanium surface selectively analysed by the sample PMT. However, as the lubricant boils away the reflection from the surface of the lubricant moves towards the titanium surface reflection and may partially overlap it. This causes a slight increase in the light measured by the PMT and is especially apparent towards the end of each run. Thus during a normal corrosion experiment the observed change in reflected light is caused by both changing color of the titanium surface and the convergence of the two reflections from the titanium and lubricant surfaces. (The lubricant absorbs visible light insignificantly.) This complication was compensated for in the analysis of the data. Since in ~6 hours all the lubricant in the cell boils away, a maximum duration of ~6 hours was imposed on all the experiments.

In addition to limiting the length of each experiment, the vapor escaping from the heated oil also interferes with incident and reflected laser illumination. Temperatures above 270°C were not practical because the large amounts of evolving oil vapor scatter the laser light. This was especially apparent when using a glove bag during the nitrogen atmosphere experiments.

Due to the corrosive properties of the heated oil, the cell cannot be closed off with a window since glass and quartz are erroded by the oil vapor that forms

a frosted surface on the window. As the oil breaks down it forms COF_2, this in turn reacts with the glass surface to form SiF_4 and CO_2.[1]

RESULTS AND DISCUSSION

It has been shown previously that perfluoropolyethers thermally decompose in the presence of oxygen producing COF_2 and CF_3COF as major products.[1-4] This reaction does not occur to an appreciable extent at temperatures below 320°C (610°F).

At temperatures below 410°C a limited oil degradation takes place. Only hydrogen terminated chains decompose. It is theorized[1] that the hydrogen end groups are more easily oxidized and that this initial oxidation leads to the breakdown of the rest of the chain. At temperatures above 410°C fluorine-terminated chains will decompose as well.

M-50 ball bearing alloy was found to accelerate the degradation of hydrogen-terminated chains.[1] Ti(4Aℓ, 4Mn) alloy accelerates the degradation to a greater extent than does the M-50 alloy. The Ti(4Aℓ, 4Mn) alloy causes chain scissions, not just oxidation of weak end groups. Chain scission is caused by the formation of AlF_3 which acts as a fluorinating agent that attacks the ether bonds in the polymers. AlF_3 is formed from R_fCOF compounds[5] in the lubricant and Al_2O_3 on the alloy surface.

The purpose of the present experiments was to determine the kinetics of the corrosion of titanium metal by hot perfluoropolyether as typified by Krytox MLO-71-6.

EFFECT OF ATMOSPHERE ON CORROSION

Virtually no titanium corrosion was observed when the sample was heated under a pure nitrogen atmosphere after the lubricant had been deoxygenated by bubbling nitrogen through the liquid. In experiment 11 (see Table I) the cell was heated

to 270°C for 90 min without any appreciable change in reflectance being observed as compared with experiment 6 where the reaction under an oxygen atmosphere at the same temperature was complete (1% of original reflectance) in 75 min.

When the cell was heated in a diminished oxygen atmosphere (as described above) the titanium surface corroded rapidly. Reflectance curves obtained were characterized by a short initial fluctuating period as the cell came up to temperature followed by an apparent first order exponential decrease in reflectance as the titanium surface corroded (see Figure 2).

Five runs were made at final temperatures ranging from 270°C down to 215°C (experiments 1 through 5) and analysed as pseudo-first order reactions. Reaction rates are expressed in terms of the variable τ in the following rate expressions:

$$\text{Reflectance} = \text{unreacted titanium} = Ae^{-t/\tau}$$

where A is the initial reflectance amplitude or initial unreacted titanium concentration and t is time in seconds. Values of τ for these experiments are listed in Table I.

The cell was also heated in an oxygen atmosphere. Reflectance curves similar to those found using a diminished oxygen atmosphere were obtained and analysed as described above. Results are shown in Table I for three different temperatures (experiments 6 through 8). Reaction rates were approximately twice as fast using oxygen as compared to diminished oxygen experiments.

In addition to being faster the oxygen atmosphere experiments appeared to corrode the titanium to a greater extent than the diminished oxygen experiments did. The reflectance during the diminished oxygen atmosphere experiments decreased to 20-30% of its original value while the reflectance for the oxygen experiments decreased to less than 2% of its original value.

From the ln τ versus reciprocal Kelvin temperature plots in Figure 3 for the unpolished O_2 rich and N_2 rich sets of experiments the Arrhenius activation energies were calculated for the reactions and found to be 3.22 kcal and 5.27 kcal respectively.

The order of the reaction was not studied further as no solvent (for example mineral oil) could be found to dilute the lubricant that did not either boil off at the high temperature used or adversely effect the titanium itself.

The possibility that the probing laser illumination might be effecting the measured corrosion rates was investigated. The laser was focused to a sharp point on the titanium surface approximately 1 mm^2 in area. The output of the laser was increased to 3 watts and the cell heated to 270°C. The titanium surface was not seen to corrode at either a greater overall rate (due to a greater laser intensity) or preferentially on the area illuminated by the laser.

CATALYSIS OF DEGRADATION BY TITANIUM CORROSION PRODUCTS

For experiments 1 through 8 a small amount of TiF_3 corrosion was left on the surface of the titanium and on the Monel walls of the cell (the Monel does not corrode but does pick up corrosion products from the side of the titanium rod). The experiments produced a reflectance versus time curve which was characterized by exponential decrease (as described above).

For experiments 9 through 12 the cell and titanium surfaces were thoroughly polished to remove all traces of corrosion. Reflectance versus time curves for these experiments showed the exponential decrease observed in the previous experiments but this was preceded by an initial induction period during which the titanium degraded very slowly (Figure 2B). The corrosion process is 3 to 4 times slower on a polished surface as compared to a surface that starts out with a small amount of TiF_3 remaining from an earlier corrosion experiment.

Apparently the corrosion products accelerate the corrosion process. The lubricant must break down into R_fCOF type molecules (e.g. COF_2 and CF_3COF) to corrode the metal; the TiF_3 may accelerate this polymer degradation process.

Thus, for the experiments with TiF_3 present initially, it appears there is a rapid degradation of oil causing a rapid corrosion of the titanium whereas with the polished rod, the induction period indicates a much slower initial oil degradation and titanium corrosion. As the oil slowly corrodes the surface, TiF_3 begins to build up which in turn accelerates the oil degradation and thereby the corrosion. Perhaps initial oil degradation involves oxidation of hydrogen-terminated weak end groups whereas degradation accelerated by the TiF_3 is chain scission.

To test these theories a simplified reaction scheme was used to generate a computer simulated reflectance curve. The first reaction is a slow degradation of hydrogen terminated chains:

$$-\underset{\underset{CF_3}{|}}{CF}-CF_2-O-\underset{\underset{CF_3}{|}}{CF}-CF_2O\cdot + \tfrac{1}{2}O_2 \rightarrow -\underset{\underset{CF_3}{|}}{CF}-CF_2-O\cdot + CF_3COF + COF_2$$

A second faster reaction involving the TiF_3 causes chain scissions:

$$-\underset{\underset{CF_3}{|}}{CF}-CF_2O-\underset{\underset{CF_3}{|}}{CF}CF_2O- + TiF_3 \rightarrow -\underset{\underset{CF_3}{|}}{CF}COF + C_2F_5CF_2O- + TiF_3$$

These fragments then degrade further into COF_2 + CF_3COF compounds.

Finally, these R_fCOF compounds react with titanium metal to form TiF_3 corrosion products. Concentration and rate constant parameters were adjusted to conform with experimental conditions and to give the best fit of the experimental data. A comparison of theory versus experiment is shown in Figure 4.

As is always true in reaction rate studies, other reaction schemes can be found that fit the data shown, but they lack the simplicity of the scheme just noted.

ANALYSIS OF REACTANTS AND PRODUCTS

An IR spectrum was run on the oil sample before and after each corrosion run, there was no change in the spectra after any of the experiments.

ESR analysis of the surface of the titanium indicated there were no radicals left on the surface.

REFERENCES

1. K. L. Paciorek, R. H. Kratzer, J. Kaufman, and J. H. Nakahara, Technical Report No. AFML-TR-77-150 to Air Force Materials Laboratory, August (1977).
2. C. E. Snyder, Jr., C. Tamborski, H. Gopal, and C. A. Svisco, Amer. Soc. Lubrication Eng., Preprint No. 78-AM-1B-2, 33rd Annual Mtg., April (1978).
3. C. E. Snyder, Jr. and R. E. Dolle, Jr., ASLE Trans. 19, 171 (1976).
4. D. Sianesi, V. Zamboni, R. Fontanelli, and M. Binaghi, Wear 18, 85 (1971).
5. The R_fCOF notation is taken from reference 1. The R_f denotes a polymer chain segment that is fully perfluorinated.

Table I. Summary of titanium metal corrosion by heated Krytox ML0-71-6

Experiment Number	Atmosphere	Temperature °C	Surface Preparation	Duration of Exp. (Min.)	Reciprocal Pseudo First Order Rate Expressed as "Tau" in sec.
1	N_2 Flush[a]	270	> 1% TiF_3[b]	75	570 ± 50
2	N_2 Flush	255	> 1% TiF_3	85	1050 ± 100
3	N_2 Flush	240	> 1% TiF_3	135	1800 ± 180
4	N_2 Flush	230	> 1% TiF_3	177	2400 ± 240
5	N_2 Flush	215	> 1% TiF_3	230	5500 ± 550
6	O_2	270	> 1% TiF_3	75	380 ± 40
7	O_2	240	> 1% TiF_3	93	970 ± 100
8	O_2	215	> 1% TiF_3	120	1430 ± 100
9	O_2	270	Polished[c]	90	1300 ± 200
10	O_2	255	Polished	115	1800 ± 180
11	N_2	270	Polished	90	———[d]
12	N_2 Flush	270	Polished	120	2000 ± 400

a) "N_2 Flush" indicates experiment was run open to the air with a fast stream of dry nitrogen flushing the surface of the oil producing a diminished oxygen atmosphere.

b) "1% TiF_3" indicates a small amount of the TiF_3 corrosion product was left on the surface of the titanium metal rod.

c) "Polished" indicates all previous corrosion was removed from the titanium rod before starting the experiment.

d) No corrosion seen in a pure nitrogen atmosphere.

Figure Captions

Fig. 1: Schematic of lubricant corrosion cell. Heating elements in the Monel walls of the cylindrical cell are not shown. Effectively, this is a double beam comparison reflectance spectrophotometer.

Fig. 2: Curve A is an experimental plot of reflectance of λ = 514 nm laser light (vertical axis) versus time for an incompletely polished titanium metal surface exposed to hot (270°C) Krytox MLO-71-6 under a diminished oxygen atmosphere. Curve B is a similar plot for a well polished titanium metal surface under the same experimental conditions.

Fig. 3: Plot of ln τ versus reciprocal Kelvin temperature. Arrhenius plots of kinetic data in Table I. Upper line is based on experiments 6 through 8 involving an oxygen atmosphere and incompletely polished titanium. The calculated activation energy E_a = 3.22 kcal. Lower line is based on experiments 1 through 5 involving a nitrogen atmosphere and incompletely polished titanium. E_a = 5.27 kcal.

Fig. 4: Comparison plot of reflectance versus time curves. Triangles are experimental data (270°C, diminished O_2 atmosphere). Black circles are computer generated using equations in the text.

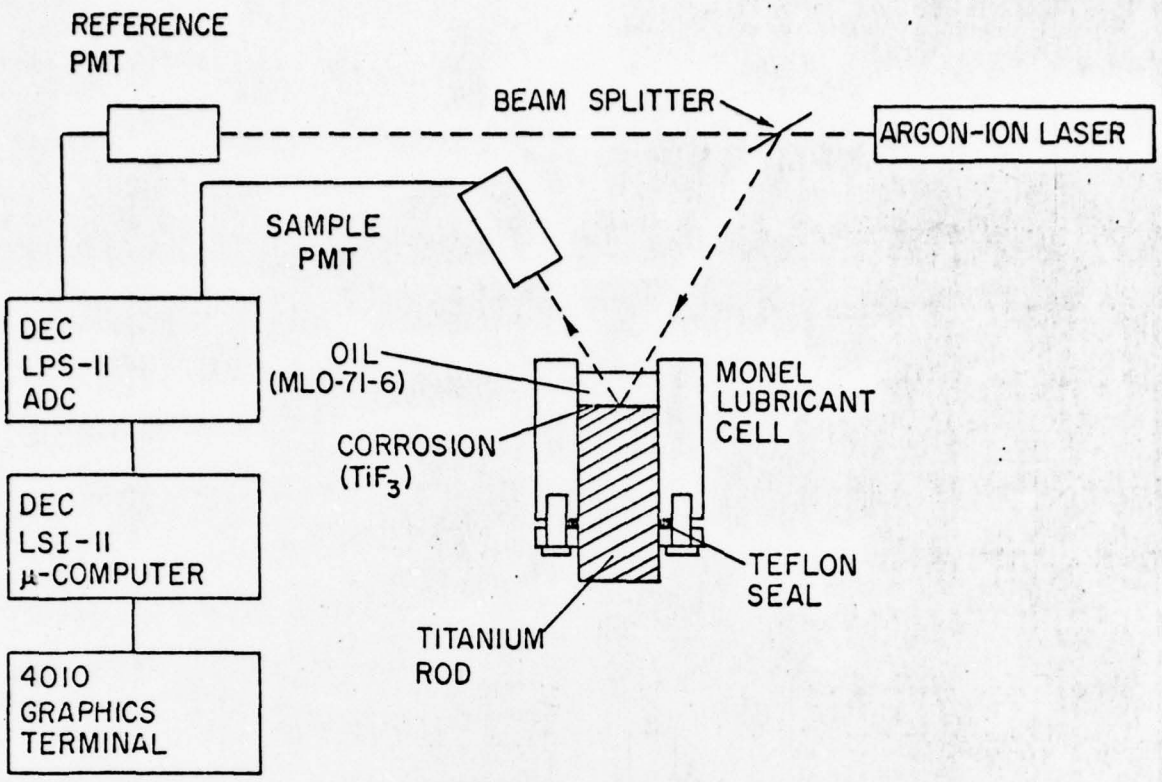
REFERENCE
PMT
BEAM SPLITTER
ARGON-ION LASER
SAMPLE
PMT
DEC
LPS-11
ADC
DEC
LSI-11
μ-COMPUTER
4010
GRAPHICS
TERMINAL
OIL
(MLO-71-6)
CORROSION
(TiF_3)
MONEL
LUBRICANT
CELL
TEFLON
SEAL
TITANIUM
ROD

FIG. 1

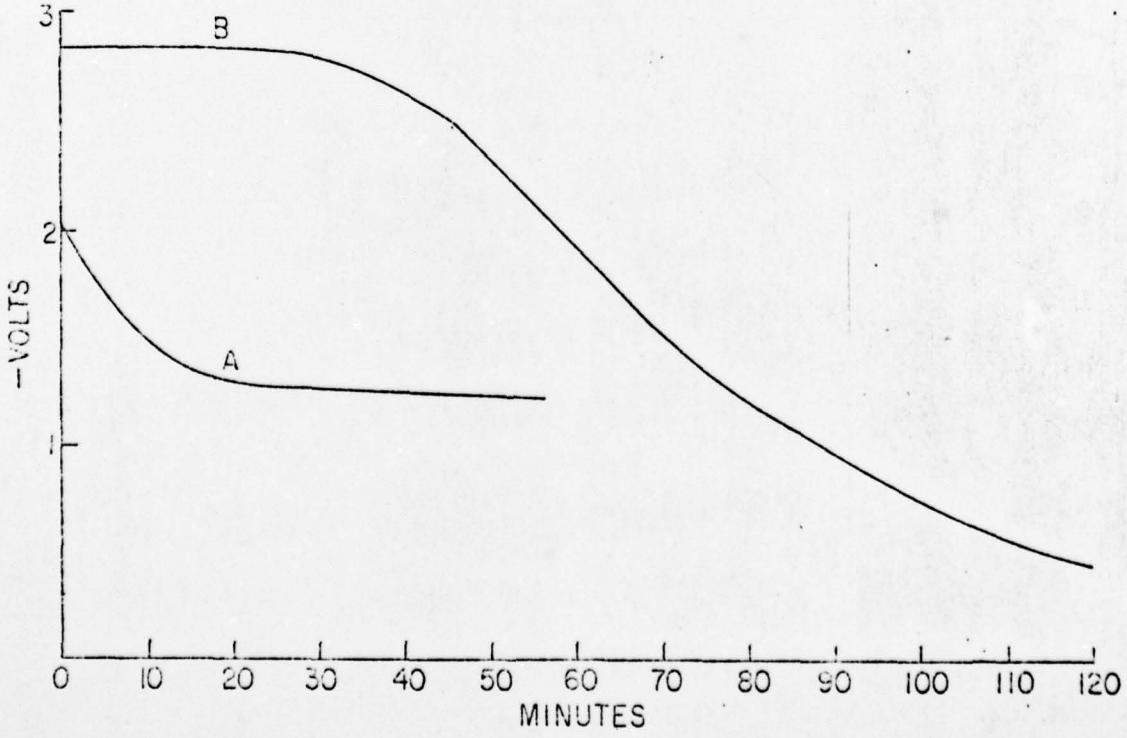
3
2
1
B
A
-VOLTS
0
10
20
30
40
50
60
70
80
90
100
110
120
MINUTES

FIG. 2

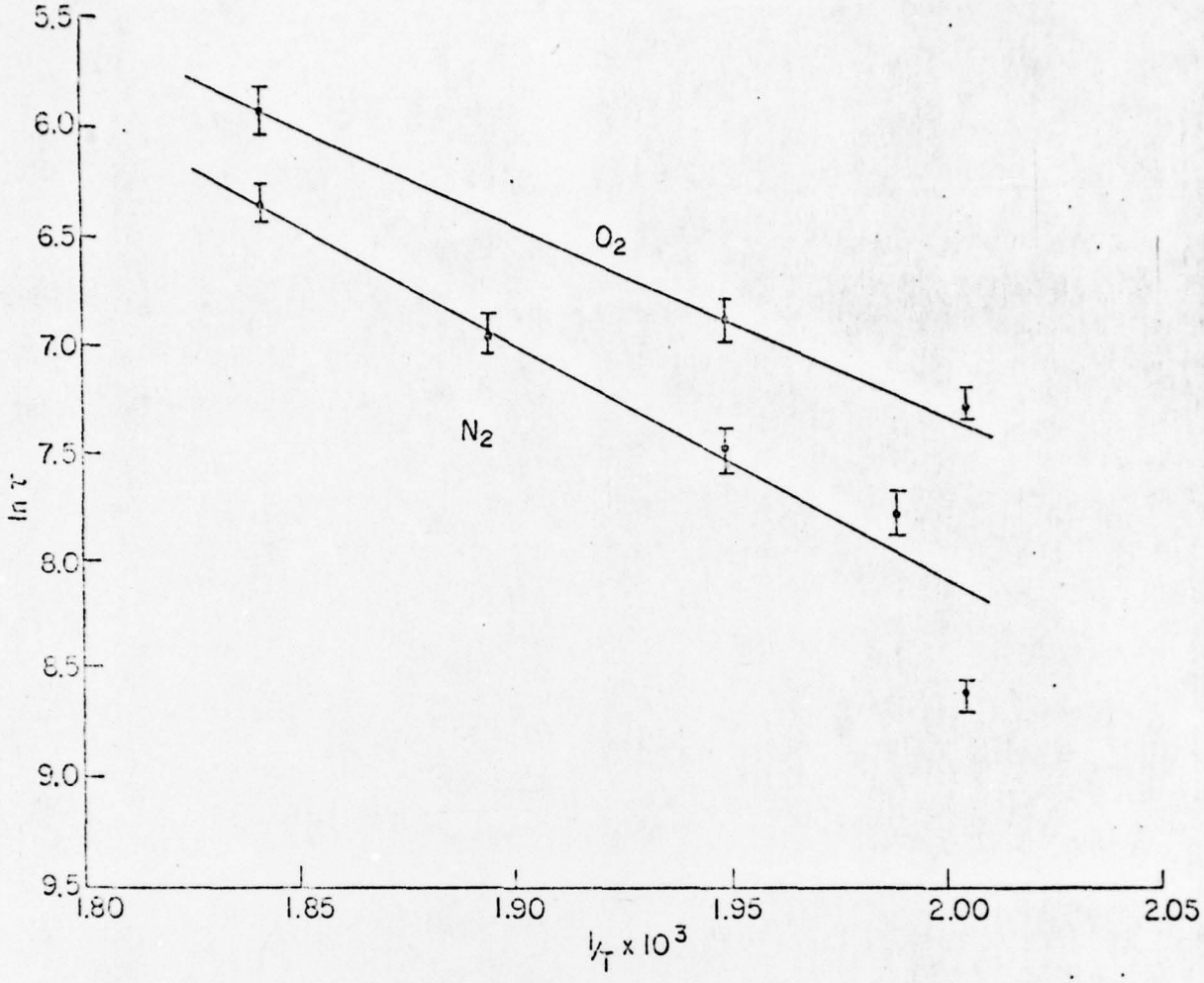
5.5
6.0
6.5
7.0
7.5
8.0
8.5
9.0
9.5
ln τ
O2
N2
1.80
1.85
1.90
1.95
2.00
2.05
1/T x 10^3

FIG. 3

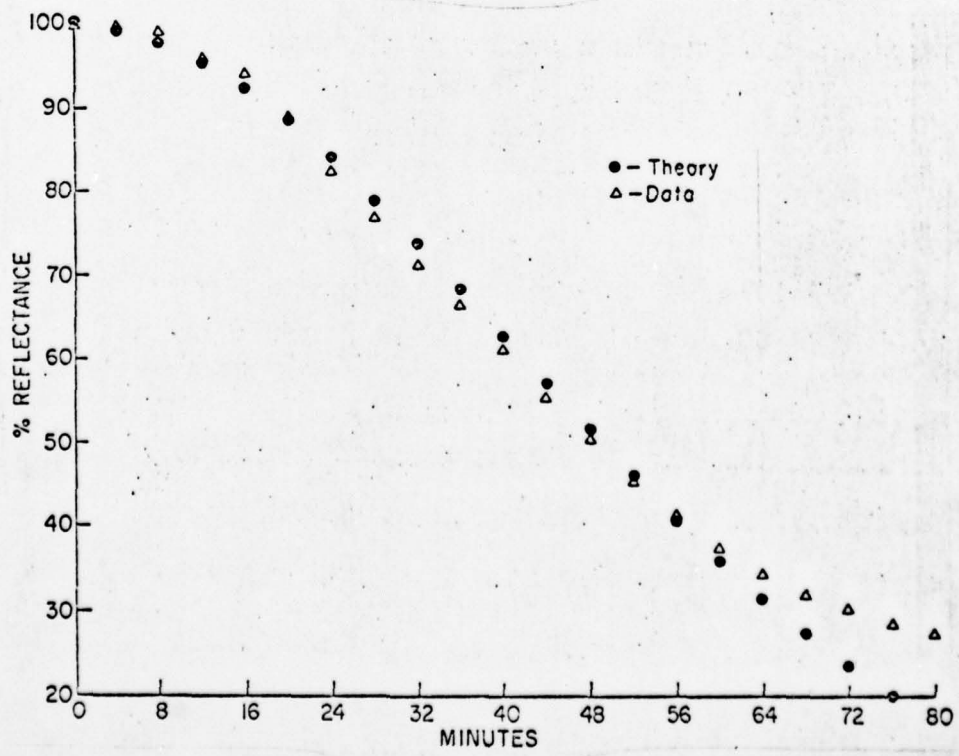
100
90
80
70
60
50
40
30
20
% REFLECTANCE
● – Theory
△ – Data
0
8
16
24
32
40
48
56
64
72
80
MINUTES

FIG. 4

Appendix II

FOURIER TRANSFORM PHOTOACOUSTIC SPECTROSCOPY

Photoacoustic spectrometers for recording visible spectra of opaque as well as practically transparent solid samples operate according to basic principles first described by Alexander Graham Bell (1,2). A visible wavelength is selected by a monochromator from the white light emitted by an arc or filament source, chopped with a rotating sector at an audio frequency (~50 Hz), and passed through a glass window onto the sample surface in an enclosed cell (3). If the surface absorbs light of the incident wavelength, electronic excitation rapidly degrades into heat by radiationless transitions, and the layer of gas in the cell in contact with the sample surface is intermittently heated at the frequency with which the light beam was chopped. The resulting sound wave in the gas is detected by a microphone located at a position in the cell where the scattered light beam cannot strike it. The signal voltage from the microphone is amplified by a lock-in amplifier that is coupled to the chopping wheel in such a way that only that part of the signal that bears a selected time relationship to the repetitive illumination intervals is amplified. Thus the lock-in amplifier can bring up to detectable levels, weak signals that would otherwise be buried in random, environmental noise.

Photoacoustic spectroscopy (PAS) has found recent use in determining the extinction coefficients of highly transparent solids and gases (4), absolute fluorescence quantum yields in liquids (5), lifetimes and mechanisms of radiationless transitions in solids (6), the band edge in semiconductors (7), the visible absorption spectrum of highly scattering fluids such as whole blood (7), the corrosion chemistry of copper intrauterine devices (8), and the near infrared to ultraviolet absorption spectrum of an inorganic linear-chain conductor (9). Other applications have included the measurement of thermal diffusivities in solids (10), the measurement of the visible absorption spectrum of the waxy cuticle (surface layer) of a plant leaf (11), the detection of tetracycline applied topically to human skin (12), a similar study of newborn rat stratum corneum (the outer most layer of the epidermis) (13), and the detection of gases evolving from the surface of a photoactivated heterogeneous catalyst (14).

A great many other studies have been made in recent years using photoacoustic spectroscopy to investigate the properties of gases (15).

Karasek's investigation of two then (1977) commercially available photoacoustic spectrometers for determining spectra of opaque specimens led him to the pessimistic conclusion that PAS would not become widely useful in studying solids until sensitive measurements are routinely possible in the infrared (16).

Intense, broadly tunable infrared emitting lasers are still not available, but even if they were, a much less expensive method of enhancing the signal to noise ratio of an infrared photoacoustic spectrometer is already available: the Michelson interferometer and Fourier transform (FT) techniques. An alternative approach is the Hadamard transform spectroscopy technique in which the spectral information is encoded in a binary code based on Hadamard matrices (17). This corresponds to an algebraic permutation of the various spectral components. In Fourier transform spectroscopy, the spectral information is encoded according to sines and cosines. Since both the Fourier transform and Hadamard transform spectroscopic techniques are multiplexing techniques, they should gain equally from any advantage in the signal to noise obtained from multiplexing spectral information in a situation where the system is detector noise limited (see below).

In September, 1977, we decided to assemble a prototype Fourier transform photoacoustic spectrometer. We applied the Fourier transform technique since the cost of commercial Hadamard transform masks is of the order (18) of $25,000, and an effective Michelson interferometer can be constructed for less than $10,000 exclusive of control electronics and computer (19). We had our prototype instrument working by April, 1978, and reported (20) a comparison of the visible FTPAS spectrum of neodymium (III) doped laser glass with a spectrum we had obtained previously (21) with a more conventional photoacoustic spectrometer. The combined throughput and multiplex advantages of the interferometer significantly reduce the data collection time and/or improve the signal-to-noise ratio.

Our prototype FTPAS apparatus did not have any applications to the research we were then funded to perform so that our instrument remains much as we first described it (20).

DESCRIPTION OF EXISTING PROTOTYPE FTPAS

The fundamental components of a Michelson interferometer are depicted schematically in Fig. 1. One possible misconception regarding the use of a Michelson interferometer at visible wavelengths is that it is difficult to obtain a sufficiently precise movement for the scanning mirror, M_1, to provide useful resolution in the absorption spectrum (Fourier transformed interferogram). This is definitely not the case. The actual reason that FT techniques are not commonplace in visible spectroscopy is that the usual visible spectrophotometer with a photomultiplier tube for a detector is source-noise-limited rather than detector-noise-limited so that FT methodology does not improve (and actually degrades) the quality of the measured spectrum.

Light from the source S is split into two beams of approximately equal amplitude. If the two beams have traversed precisely the same effective path length in returning from the mirrors to the beamsplitter B, they will be in phase with one another and will interfere constructively. In order to provide exactly equivalent paths in both arms of the interferometer, a compensating plate of material identical to the beamsplitter substrate but without the beamsplitting coatings, is placed in the appropriate arm of the interferometer. This compensates for any wavelength dependent dispersion of the beam splitter substrate. Any difference in path length is referred to as retardation. If the effective path length on reaching B differs by a half integral wavelength distance, the beams from the two arms will be out of phase and will destructively interfere with each other. We will refer to the bright areas of constructive interference as "bright fringes".

The actual beam path for light passing through an interferometer may be more easily visualized with the aid of Fig. 2 which shows an equivalent arrangement for the mirrors in Fig. 1. The case illustrated is for one mirror, M_1, being

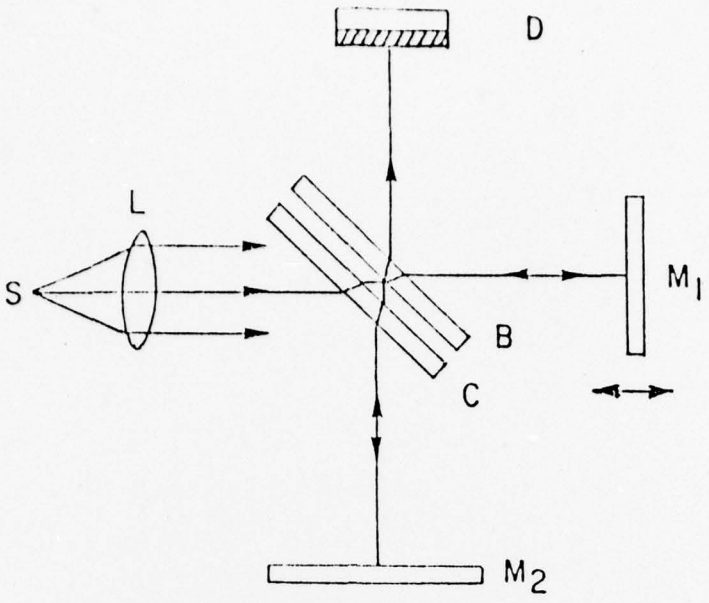

Fig. 1. Schematic of a Michelson interferometer. S in the FTPAS is a 100 watt tungsten iodide lamp. M_1 is a movable front surface mirror, L is a collimating lens, and M_2 is a "stationary" front surface mirror. M_1 flutters to provide the analog of beam chopping in ordinary PAS, B is a half silvered beam splitter, C is a compensating plate, and D is the detector (a piezoelectric transducer, microphone, photomultiplier tube, or the eye of an observer). The crosshatching on D depicts a sample material that in the case of a piezoelectric detector is glued to the piezoelectric.

nearer to the beam splitter than the other mirror, M_2. The virtual images of the source, S_1, appearing in each mirror are identified by the appropriate subscripts. If the path lengths in the two arms differ by distance d, then the virtual sources are separated by 2d, since the path is traversed twice by the beam on its way to and from the mirrors. The appropriate arrangement of the mirrors in the interferometer used in FTPAS is that in which the mirrors are perfectly perpendicular. This is equivalent to the parallel positioning in Fig. 2 and contrasts with some other interferometric geometries in which one mirror is canted with respect to the other.

If a perfectly aligned Michelson interferometer is illuminated with a monochromatic light source and an observer places his eye at the output of the interferometer, looking back toward the beam splitter and source (Fig. 2), he will observe circular interference fringes. Although all rays of light reflected normal to the mirrors will be in phase, rays reflected at any angle will not, in general, be in phase. Figure 2 shows that for any given angle θ the path difference is given by $2d \cos \theta$. Since the rays must be parallel for interference to occur, θ must be the same for both rays coming from either virtual source, S_1 or S_2. The rays will reinforce each other to produce maxima or bright fringes for those angles θ which satisfy the relationship:

$$2d \cos \theta = m \lambda \qquad (1)$$

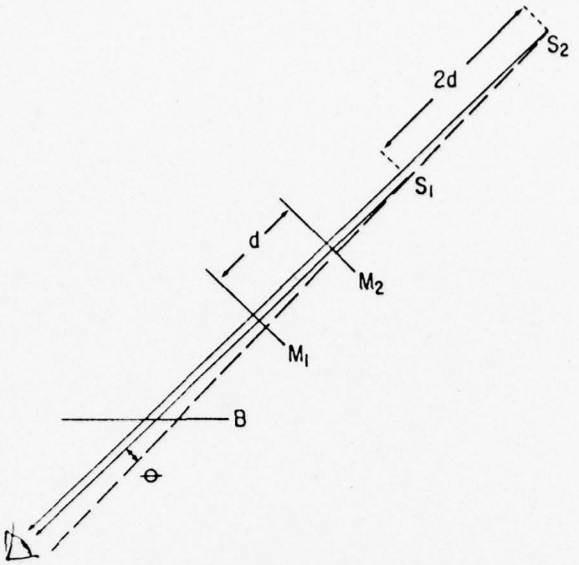

Fig. 2. Schematic of light paths in a Michelson interferometer. Compensating plate has been omitted for clarity. See text for complete description.

Here d is the mirror separation, λ is the wavelength, m is an integer, and θ is a constant which produces a circular fringe. If m is half integer, then destructive interference occurs and a dark fringe results. At the center of the fringe, θ is zero and $\cos \theta = 1$, so that equation 1 becomes

$$2d = m \lambda \qquad (2)$$

In order for m to change by unity, d must change by λ. As the two virtual sources S_1 and S_2, approach each other, the angle θ must decrease and the fringes become more widely spaced. At a critical position, there is only one dark fringe visible. This happens when M_1 and M_2 are exactly coincident, since for this position the path difference is zero for all angles of incidence.

If white light is used to illuminate the interferometer, no fringes will be seen except very close to zero path difference between the two mirrors. At zero path difference there will be a dark central fringe, bordered by eight to ten colored fringes. That there are only a few fringes visible with white light is easily accounted for by recalling that all wavelengths between ~400 and 750 nm are contained in visible light. There will be coincidence of various wavelength fringes only for d = 0, since the fringe spacing varies according to the wavelength with fringes for longer wavelengths being more widely spaced. Clearly the fringes of different colors will begin to separate on either side of zero producing impure colors. After eight or ten fringes so many colors are present that the resultant is essentially white. Interference is still occurring, but the eye is not sensitive enough to resolve the variations in intensity.

Two techniques are useful for locating the zero path difference position of the mirrors. One of these is to use a monochromatic light source and locate that position of the two mirrors for which the central fringe has expanded to fill the field of view as mentioned above. Another is to use a monochromatic light source that is actually a doublet such as the sodium D line. The interference produced by two closely spaced spectral lines will be a sine wave whose amplitude varies at some lower sinusoidal frequency. The output of the interferometer is focused on a photomultiplier and the path length difference of the two mirrors is varied in some uniform manner (i.e. a sawtooth motion). If the out-

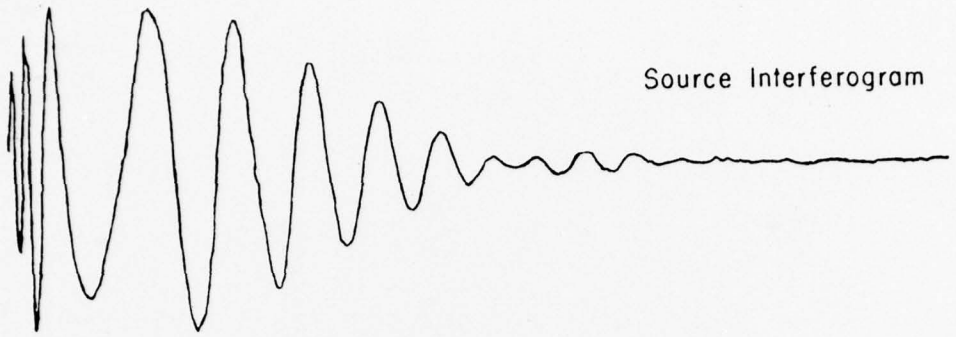

Fig. 3. Typical interferogram of a broadband light source. A schematic of the trace observed on an oscilloscope screen when the PMT voltage (vertical) is displayed versus time (horizontal). The time axis corresponds to changes in the mirror position M_1 of Fig. 1 about equal path difference in the arms of the interferometer.

put of the photomultiplier is displayed on an oscilloscope, the sinusoidal envelope which contains a high frequency sinusoidal modulation is observed and as the path lengths of the two arms approach equality, the modulation depth of the higher frequency sinusoidal modulation in the envelope increases. If the interferometer is adjusted to produce a maximum modulation depth, zero path difference has been located. If a white light is then used to illuminate the interferometer, the photomultiplier should detect the expected eight to ten fringes and present the typical interferogram of a broadband source, see Fig. 3.

The amount of light passing through the interferometer will remain essentially a constant if averaged over the entire field of view. Only the central (Airy) disc will vary as the interferogram of the source. For this reason, one places an aperture at the focus of the interference pattern and only allows the central portion of the fringe pattern to fall on the detector.

Since Fourier transform photoacoustic spectroscopy (FTPAS) still requires a modulation of the optical signal at the detector, the source intensity must be modulated in some manner. This may be accomplished by a technique known as phase modulation (22). This method, also known as internal modulation, requires a slow scanning interferometer, usually employing the step and integrate method of traversing the moving mirror. At discrete positions of the moving mirror the beam is modulated not by a chopper, but by periodically varying the retardation of the moving mirror by a small amount. This small variation in the retardation or jitter, if made infinitesimally small, would result in the measured interferogram being the first derivative of the interferogram. In practice, even with finite jitter amplitudes, a phase modulated interferogram is a very good approximation to the first derivative of the amplitude modulated interferogram. An added benefit of a phase modulated interferogram is that the large DC offset which otherwise must be measured is eliminated. This DC offset corresponds to white light which does not interfere with itself in the interferogram and presents a large background. Since the first derivative of an amplitude modulated interferogram is a sine function, the spectrum can then be computed from the interferogram by sine transform (22).

Another modulation technique, known as rapid scan, takes advantage of the fact that if the input to an interferometer is monochromatic and the mirror is moved at a constant vellocity, the ouput of the detector varies sinusoidally with a frequency given by $f_\sigma = 2V\sigma$ (Hz). In this equation, V is the mirror velocity in cm./sec., and σ is the wave number of the light in cm^{-1}. The factor of two appears because if the mirror moves at velocity V, the retardation is changing at a rate of 2V. Thus each wavelength is modulated at its own characteristic frequency. The rapid scan technique would be advantageous for kinetic measurements, but has no special advantages (except in the smaller dynamic range required in the rapid scan electronics) for the determination of absorption spectra of static or nearly static sample systems.

In photoacoustic spectroscopy, signal amplitude increases only when absorption occurs. Thus, photoacoustic spectra will be absorption spectra as opposed to FTIR spectra which are transmission spectra. FTPAS interferograms should then show modulation at high values of retardation as well as near zero retardation. This comes about as a consequence of the properties of Fourier transforms which cause very broad general feature information to be collected at low retardation, with narrow and sharp features ("high frequency") to be collected at higher retardation.

The entire interferometer is mounted on a 96 x 80 x 20 cm granite slab which rests on a ~15 cm thick bed of polyurethane foam. The combination of approximately 300 kilograms of granite and 15 cm of foam effectively decouples the interferometer from mechanical and seismic events in the building. The framework of the interferometer is one inch diameter stainless stell rod and is somewhat sensitive to thermal expansion caused by heating from the light source. The 5 cm, $\frac{\lambda}{20}$ (full aperture) mirrors (Pyramid Optical Corp.) are mounted in Star-Gimbal mounts (Burleigh). The visible wavelength beam splitter and compensating plate are both $\frac{\lambda}{20}$ (parallel to one second of arc) with 5 cm full aperture (Pyramid Optical Corp.). The beam splitter is located in a 45° optical mount (Burleigh) which is supported by a Star-Gimbal mount for adjustment. The fixed mirror is also the phase modulating mirror. In order to accomplish the phase modulation the mirror is mounted on a PZAT-90 (Burleigh) piezoelectric mount. There is sufficient linear motion available (~10 micrometers/1000 V) from this mount to drive several orders of visible fringes.

Figure 4 is a schematic of the step and integrate FTPAS apparatus we have described in the preceding paragraphs.

A representative interferogram (Fig. 5) and transformed absorbance spectrum (Fig. 6) of neodymium (III) doped laser glass suggest the potential utility of FTPAS for obtaining high resolution spectra in analytical chemistry. In this case the FT feature of the experiment greatly speeds the accumulation of data (20): The ordinary PAS spectrum, curve b of Fig. 6, required 90 minutes to collect with a 450-W Xenon arc lamp. The FTPAS spectrum, curve a of Fig. 6, was collected and transformed in less than 4 minutes using only a 100-W tungsten-iodide lamp as the light source.

The rough correspondence of the three neodymium glass spectra in Fig. 6 is encouraging, but it is important to determine the cause or causes of the obvious discrepancies. Probably the most important of these causes, yet to be investigated in detail, are phase errors in the measured interferogram. As stated earlier, linear motion of the PZAT-90 was assumed (i.e. constant velocity for the phase modulation method and linear voltage response for the step and integrate

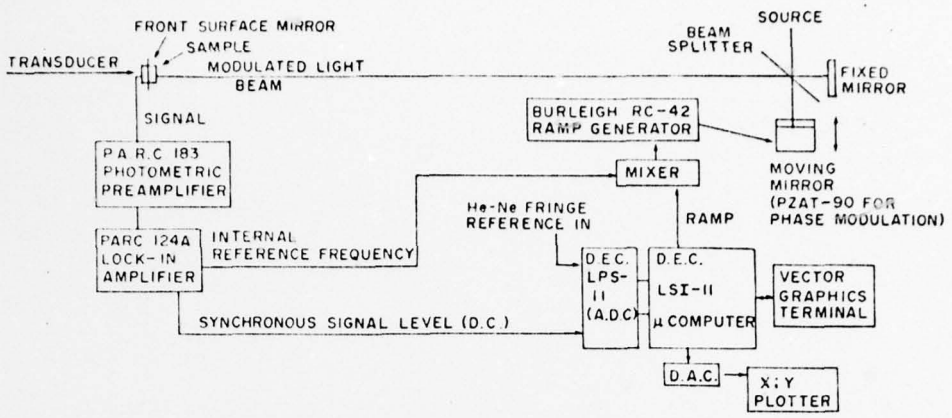

Fig. 4. Schematic of a step and integrate Fourier transform-visible-photoacoustic spectrometer. The Michelson interferometer is in the top right-hand corner.

method.) In fact, this motion is linear to an accuracy of about 5%. If not taken account of, this slight nonlinearity of motion will lead to a non-linear wavelength scale in the resulting spectrum. There are several avenues available to correct for such an effect. Burleigh Instruments Inc. now markets a new driver (RC-43) which will reduce the nonlinearity of motion by an order of magnitude to about 0.5%. On the other hand, a correction function to be used in the numerical transform could be constructed from a detailed investigation of interferograms resulting from the use of a monochromatic light source. If the interferometer is illuminated with monochromatic light, the phase modulated output is a sinusoidal variation, the frequency of which depends on the wavelength of light used. Nonlinearities in the mirror velocity result in a varying modulation frequency. Where the mirror is moving faster than average, this sinusoidal frequency is higher. Where the mirror is moving slower than average, the frequency is lower. By studying these variations, a true velocity profile for the mirror can be derived. Of course, a nonlinear voltage-mirror step relationship could be mapped in a similar fashion.

Another phase error may arise from imperfect alignment of the compensating plate of the interferometer. This results in the position of zero path difference for each wavelength not occurring at the same mirror position.

If the absorption spectrum of the particular sample is not flat across the visible region, each wavelength is being absorbed at some depth in the sample characteristic of the absorption at that wavelength. (The wavelength that is least strongly absorbed penetrates the sample surface to the greatest depth.) As the resulting acoustic waves travel through the sample toward the attached piezoelectric transducer, mutual interference might occur between the waves launched from differing distances beneath the surface at differing acoustic frequencies.

There are basically two techniques for mathematically correcting general phase errors (23,24) in a distorted interferogram. In a perfect interferogram the data collected are either antisymmetric or symmetric about the zero path difference (ZPD) position of the mirror corresponding to whether an internal modulation was or was not used. In practice, this fact is used to advantage by sampling the interferogram on one side of ZPD only, thereby increasing the path difference, and hence the resolution, for a given distance of mirror motion. Phase errors in an interferogram are manifested by the lack of symmetry about ZPD. If the interferogram is sampled for equal intervals on either side of the

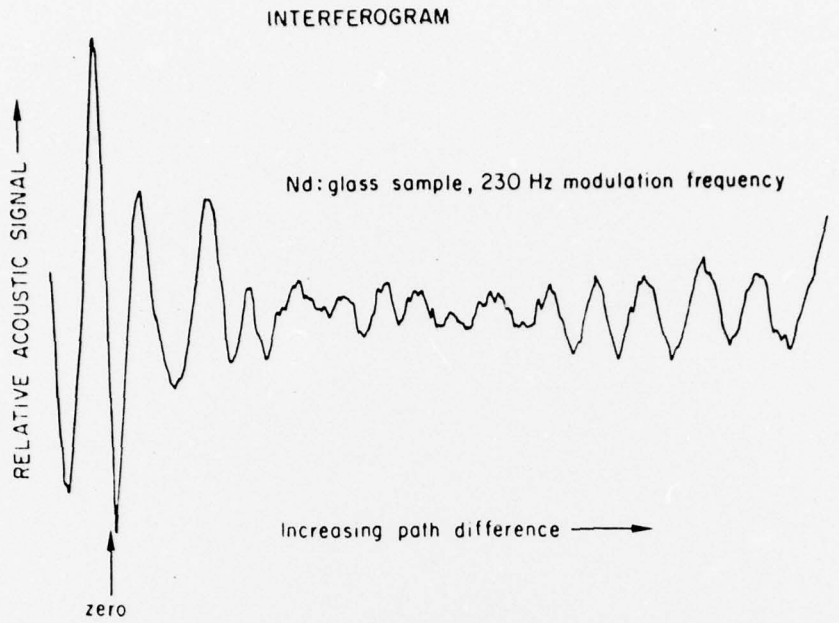

Fig. 5. Photoacoustic interferogram of Nd:glass sample.

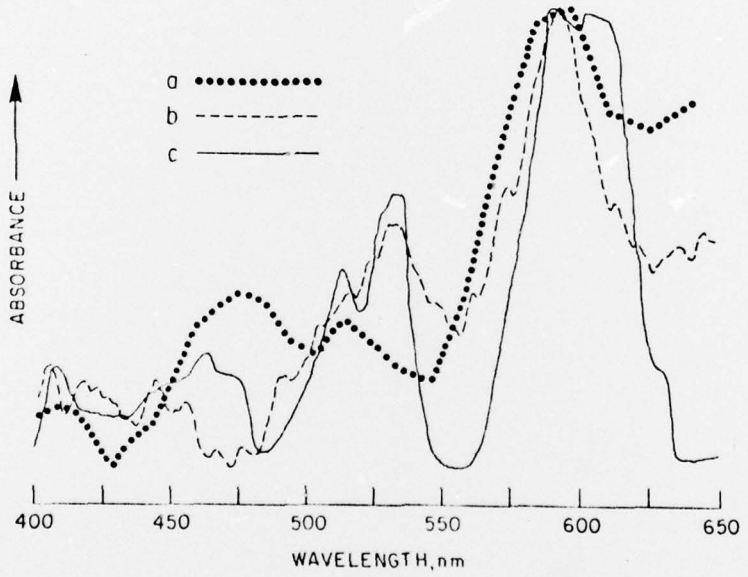

Fig. 6. Absorption spectra of Nd:glass samples. Curve a calculated from the interferogram of Fig. 5. The spectrum has not been source normalized (i.e. signal has not been divided by light source intensity at each wavelength). The interferogram was based on samples taken at 256 equally spaced mirror positions. The spectral resolution is 850 cm^{-1} or ~20 nm @ λ = 500 nm. Curve b is a dispersive PAS spectrum[21] of the same sample. Curve c is a portion of a typical absorption spectrum of another Nd:glass sample taken from the literature (K. Hauptmanova, J. Pantoflicek, and K. Patek, Phys. Stat. Sol., 9, 525 (1965).)

ZPD position, the phase errors are essentially cancelled in the resulting two sided transformation. However, this has the distinct disadvantage of reducing the effective total retardation (resolution) in half compared to an interferogram collected on one side of the ZPD position only. Both techniques of phase correction use a similar scheme, only differing in whether the correction is applied to the data before or after numerical transformation of the interferogram.

In each correction scheme a correction function is constructed by taking a relatively few data points (compared to the total number of points in the interferogram, typically 5-10% of the total) centered about the ZPD position and transforming to get a spectrum. The fact that phase errors are present results in this spectrum being complex as opposed to a purely real or imaginary spectrum resulting from a symmetric or antisymmetric interferogram. From this complex spectrum a phase function can be constructed which is a measure of how much phase error is actually present, this function being identically zero for a perfect interferogram. Because the two sided phase correction interferogram was sampled at the same spacing as the full interferogram, it covers the same spectral range. The phase correction function can now be smoothed by interpolation to have the same number of data points as the full one sided interferogram and applied to it in such a manner as to compensate for the phase errors actually present. While the finite number of data points used and truncation effects in this scheme give rise to an imperfect spectrum, application of this method in an iterative fashion can yield any desired degree of improvement.

While the technique allows one to essentially use a one sided interferogram, and thus get the maximum resolution for a given mirror motion, it also allows detailed examination of phase shifts occurring in the sample. Using the above phase correction scheme with a blackbody detector such as a blackened piezoelectric detector, one is measuring the instrumental phase spectrum characteristic of the instrument. By comparing this phase spectrum with the phase spectrum obtained with a sample attached to the transducer, a phase spectrum of the sample is obtained. In principle, this allows a calculation of the absorption depth for each wavelength and some indication of whether the acoustic interference alluded to earlier is in fact significant.

In order to derive an accurate wavelength scale, one conventionally references the sample interferogram to an interferogram obtained using a monochromatic source such as a laser. To date, our instrument does not incorporate such a laser referencing system.

Another problem to be addressed is the sensitivity of the detector. While a microphone is inherently more sensitive than a piezoelectric crystal, there appear to be fundamental problems in using a microphone as an FTPAS detector. The phase delay due to the sound wave propagation thru the intermediate gas medium interacts with the Fourier transform modulation encoding to give severe measurement problems. As the microphone's sensitivity is typically a function of frequency, in a rapid scan experiment where there is a range of frequencies present this non-constant response must be accounted for.

REFERENCES AND NOTES

1. A. G. Bell, Proc. Am. Assoc. Adv. Sci., 29, 115 (1880).

2. A. G. Bell, Phil. Mag., 11, 510 (1881).

3. See, for example, J. F. McClelland and R. N. Kniseley, Appl. Optics, 15, 2967 (1976).

4. H. S. Bennett and R. A. Forman, Appl. Optics, 15, 1313, 2405 (1976); J. Appl. Phys., 48, 1217 (1977); A. Hordvik and H. Schlossberg, Appl. Optics, 16, 101 (1977); A. Hordvik and L. Skolnik, Appl. Optics, 16, 2919 (1977).

5. W. Lahman and H. J. Ludewig, Chem. Phys. Lett., 45, 177 (1977); M. J. Adams, J. G. Highfield, and G. F. Kirkbright, Anal. Chem., 49, 1850 (1977).

6. L. D. Merkle and R. C. Powell, Chem. Phys. Lett., 46, 303 (1977); J. C. Murphy and L. C. Aamodt, J. Appl. Phys., 48, 3502 (1977); M. G. Rockley and J. P. Devlin, Appl. Phys. Lett., 31, 24 (1977); R. G. Peterson and R. C. Powell, Chem. Phys. Lett., 53, 366 (1978).

7. A. Rosencwaig, Anal. Chem., 47, 592A (1975).

8. K. M. Lewis, R. D. Archer, A. P. Ginsberg, and A. Rosencwaig, Contraception, 15, 93 (1977).

9. A. Rosencwaig, A. P. Ginsberg, and J. W. Koepke, Inorg. Chem., 15, 2540 (1976).

10. M. J. Adams and G. F. Kirkbright, Analyst, 102, 281 (1977).

11. M. J. Adams, B. C. Beadle, A. A. King, and G. F. Kirkbright, Analyst, 101, 553 (1976).

12. S. D. Campbell, S. S. Yee, and M. A. Afromowitz, J. Bioengineering, 1, 185 (1977).

13. A. Rosencwaig and E. Pines, Biochim. Biophys. Acta, 493, 10 (1977).

14. R. C. Gray and A. J. Bard, Anal. Chem., 50, 1262 (1978).

15. M. B. Robin and N. A. Kuebler, J. Am. Chem. Soc., 97, 4822 (1975); L. A. Farrow and R. E. Richton, J. Appl. Phys., 48, 4962 (1977).

16. R. W. Karasek, Research/Development, Sept., 1977, p. 38.

17. A. G. Marshall and M. B. Comisarow, Anal. Chem., 47, 491A (1975); M. Harwit in *Transform Techniques in Chemistry*, P. R. Griffiths, ed., Plenum Press, New York, N.Y., 1978, Chapter 7.

18. A. J. Bard, private communication.

19. W. K. Yuen and G. Horlick, Anal. Chem., 49, 1446 (1977).

20. M. M. Farrow, R. K. Burnham, and E. M. Eyring, Appl. Phys. Lett., 33, 735 (1978).

21. M. M. Farrow, R. K. Burnham, M. Auzanneau, S. L. Olsen, N. Purdie, and E. M. Eyring, Appl. Optics, 17, 1093 (1978).

22. J. Chamberlain, Infrared Phys., 11, 25 (1971).

23. M. L. Forman, W. H. Steel, and G. A. Vanasse, J. Opt. Soc. Am., 56, 59 (1966).

24. R. B. Sanderson and E. E. Bell, Applied Optics, 12, 266 (1973).